

Technical Note

Open Access



Nanostructural design of superstrong metallic materials by severe plastic deformation processing

Ruslan Z. Valiev^{1,2} 

¹Ufa University of Science and Technology, Ufa 450008, Russia.

²Saint Petersburg State University, St. Petersburg 199034, Russia.

Correspondence to: Prof. Ruslan Z. Valiev, Ufa University of Science and Technology, 12 K. Marx Str., Ufa 450008, Russia. E-mail: ruslan.valiev@ugatu.su

How to cite this article: Valiev RZ. Nanostructural design of superstrong metallic materials by severe plastic deformation processing. *Microstructures* 2023;3:2023004. <https://dx.doi.org/10.20517/microstructures.2022.25>

Received: 7 Sep 2022 **First Decision:** 23 Sep 2022 **Revised:** 10 Oct 2022 **Accepted:** 2 Nov 2022 **Published:** 10 Jan 2023

Academic Editors: Daolun Chen, Yandong Wang **Copy Editor:** Fangling Lan **Production Editor:** Fangling Lan

Abstract

Ultrafine-grained (UFG) metallic materials processed by severe plastic deformation (SPD) techniques often exhibit significantly higher strengths than those calculated by the well-known Hall-Petch equation. These higher strengths result from the fact that SPD processing not only forms the UFG structure but also leads to the formation of other nanostructural features, including dislocation substructures, nanotwins and nanosized second-phase precipitations, which further contribute to the hardening. Moreover, the analysis of strengthening mechanisms in recent studies demonstrates an important contribution to the hardening due to phenomena related to the structure of grain boundaries as a non-equilibrium state and the presence of grain boundary segregations. Herein, the principles of the nanostructural design of metallic materials for superior strength using SPD processing are discussed.

Keywords: Nanostructural design, severe plastic deformation, ultrafine-grained materials, superior strength

INTRODUCTION

Although several factors determine the strength properties of pure metals and alloys, the average grain size usually plays a significant role in their mechanical properties^[1,2]. In particular, the dependence of the strength of polycrystalline materials on the average grain size d is usually described by the Hall-Petch equation, according to which the yield stress σ_{YS} is depicted as follows:



© The Author(s) 2023. **Open Access** This article is licensed under a Creative Commons Attribution 4.0 International License (<https://creativecommons.org/licenses/by/4.0/>), which permits unrestricted use, sharing, adaptation, distribution and reproduction in any medium or format, for any purpose, even commercially, as long as you give appropriate credit to the original author(s) and the source, provide a link to the Creative Commons license, and indicate if changes were made.



$$\sigma_{YS} = \sigma_0 + k_{HP}d^{-1/2} \quad (1)$$

where σ_0 is the lattice friction stress and k_{HP} is the Hall-Petch coefficient. According to Equation (1), the strength of the material increases with decreasing average grain size.

Based on this connection, there is significant interest in achieving ultrafine-grained (UFG) structures in metallic materials with an average grain size of less than 1 μm and predominantly high-angle grain boundaries, which may be implemented by using severe plastic deformation (SPD) processing techniques^[3-5].

For this purpose, at present, the most popular SPD processing techniques are equal-channel angular pressing (ECAP) and high-pressure torsion (HPT). The deformation processing of materials by SPD was the first key step that initiated comprehensive studies of the mechanical properties of bulk nanomaterials and is now the basis for their innovative applications (see reviews and books on this topic)^[5-10].

The past two decades have witnessed detailed analyzes of the effect of reducing the grain size to the nanoscale on the strength of materials. Although many studies have observed an increase in strength with decreasing grain size following Equation (1), this relationship is often violated for nanosized grains (less than 100 nm). Thus, the Hall-Petch curve deviates from the linear relationship at lower stress values and its slope k_{HP} becomes negative (curve 1, [Figure 1](#))^[2]. This problem has been extensively analyzed in many experimental and theoretical studies. In addition, several recent studies have shown that UFG materials may exhibit significantly higher strengths than that predicted by the Hall-Petch relation for the range of ultrafine grains (curve 2, [Figure 1](#))^[5,6]. The nature of such superstrength may be related to the influence of various nanostructural features observed in SPD-processed metals and alloys located in the grain interior (dislocation substructures, nanosized particles of secondary phases and nanotwins) and at grain boundaries^[10].

In this regard, the task herein is to analyze the nature of the superstrength of UFG materials and various strengthening mechanisms, including both the known ones related to the presence of nanoparticles and other nanostructural features and the new ones related to the influence of grain boundary structures in UFG materials.

EXPERIMENTAL OBSERVATIONS

In the last decade, a number of studies on the strength properties of various nanostructured metals and alloys, including Al alloys^[11,12], steels^[13,14] and titanium materials^[15], have been performed in our laboratory in collaboration with colleagues from other institutions. In all cases, a significant increase in the strength of the material was observed during grain refinement by SPD techniques, with yield stress values significantly exceeding the values calculated by the Hall-Petch equation. This is illustrated in [Figure 2](#)^[11] for the yield stress values of the UFG Al alloys 1570 and 7475 with grain sizes of ~ 100 nm, which are significantly higher than the Hall-Petch ratio calculations for closely related Al alloys with similar grain sizes.

It is important that in all these and our other works^[16-19], the formation of nanoclusters and solute segregations at grain boundaries was observed along with the formation of the UFG structure. This is clearly seen, for example, when studying the SPD-processed alloys with the use of three-dimensional atom probe tomography [[Figure 3](#)]^[12], as well as in [Figure 4](#), which demonstrates observations of the nanostructural features of the alloy 7075 after HPT at two different temperatures (room temperature and 200 °C)^[20].

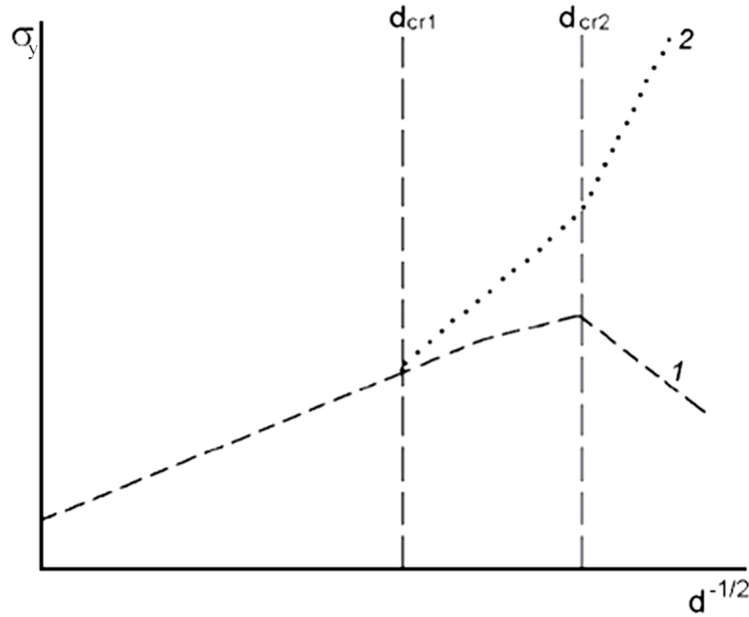


Figure 1. Two types of Hall-Petch slopes within different characteristic length scales: d_{cr1} - grain size, below which the contribution of nanostructural features (nanoparticles, substructure and others) becomes significant in the strengthening of SPD-processed materials; d_{cr2} - grain size, below which the contribution of grain boundary segregation and non-equilibrium grain boundaries becomes significant in UFG materials. Reproduced with permission, Copyright 2013, John Wiley and Sons^[5].

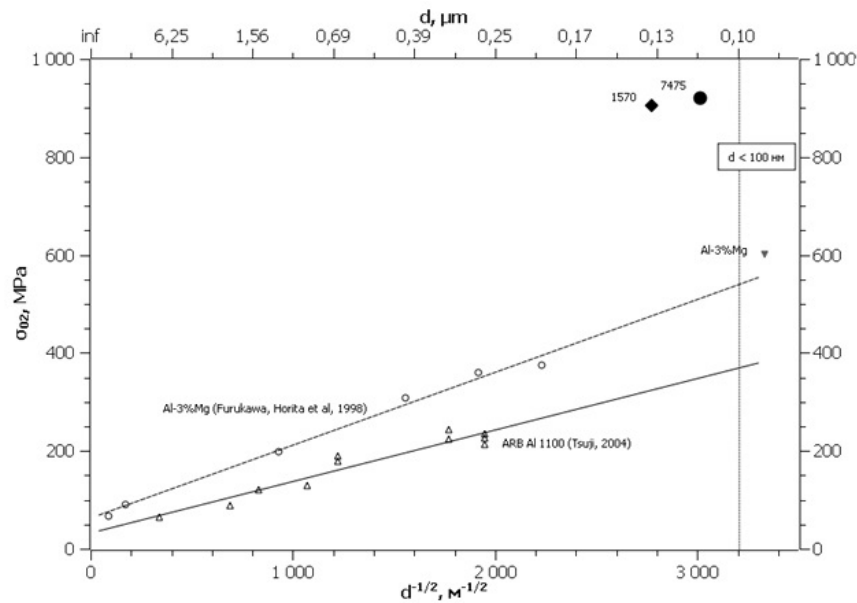


Figure 2. Hall-Petch relationships for Al 1100 and Al-3%Mg supported by the yield stress of nanostructured alloys Al-3%Mg, 1570 and 7475. Reproduced with permission, Copyright 2010, Elsevier^[11].

This study pays special attention to experiments achieving a high-strength state in commercially pure (CP) Ti Grade 4 subjected to processing by ECAP and HPT. The material (composition, wt.% Fe - 0.5, O - 0.4, C - 0.08, N - 0.05, H₂ - 0.015 and Ti - base) is favored by medical professionals for its biocompatibility and is a popular material for medical applications. CP Ti is widely used for implants because its strength is crucial

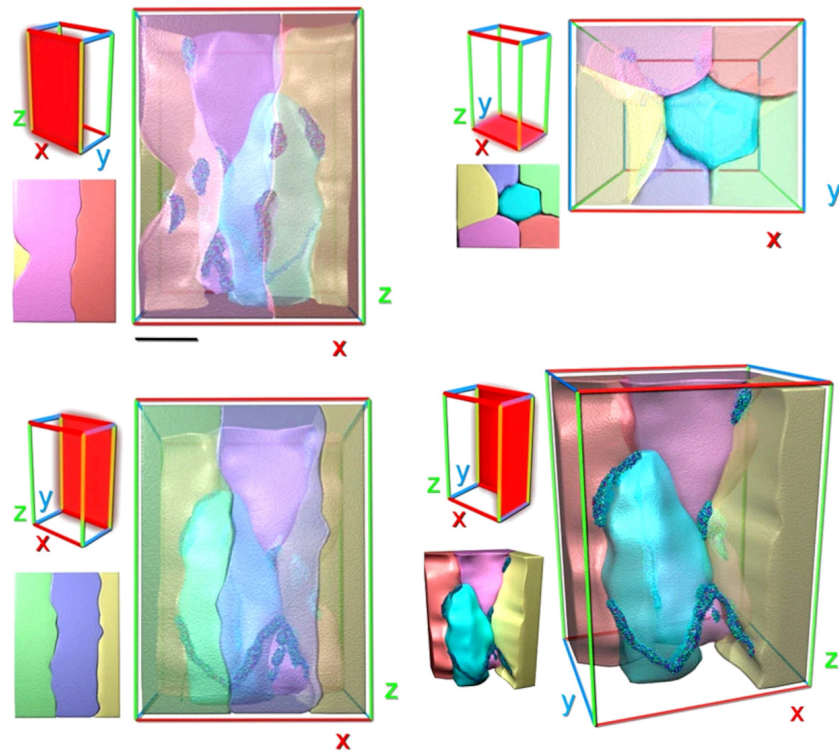


Figure 3. Tomographic view of nanostructural architecture in HPT 7075 alloy. Lineal and node solute structures are observed to occur at grain boundary interfaces and junctions. Reproduced with permission, Copyright 2010, Nature Publishing Group^[12].

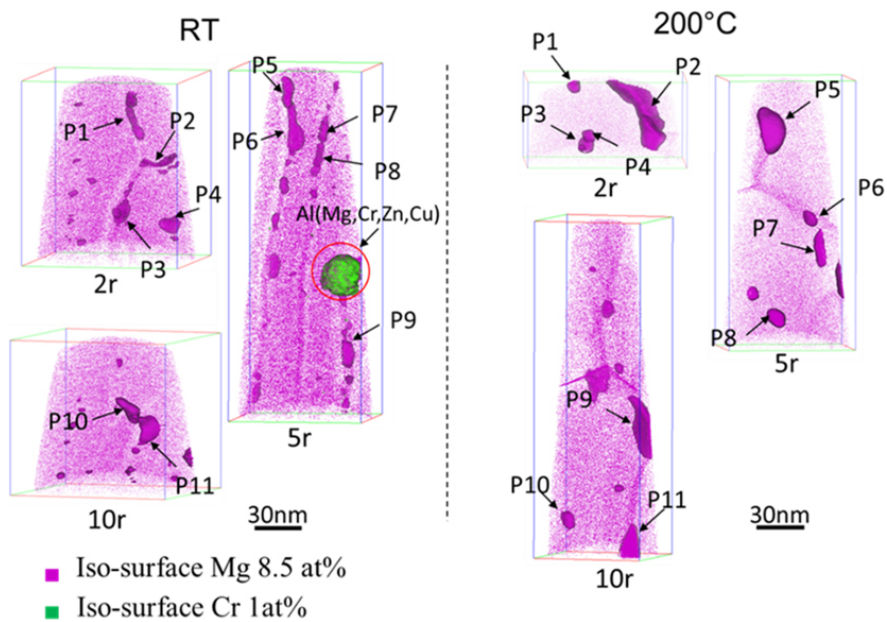


Figure 4. Three-dimensional reconstructed Mg atom maps of AA7075 samples processed by HPT in different conditions, with precipitates defined by iso-concentration surfaces at 8.5 at.% Mg (in pink) and 1.0 at.% Cr (in green). Reproduced with permission, Copyright 2018, Elsevier^[20].

for manufacturing implants of improved design with increased osseointegration^[21]. The details of Ti Grade 4

processing, including HPT in different regimes and annealing procedures [Table 1], are provided in our previous work^[22]. Table 1 also shows the structural parameters of Ti measured by X-ray and TEM analysis after processing.

Figure 5 shows the stress-strain engineering curves of the samples during tensile tests. In the initial state, the character of the curve is typical for the materials obtained by hot rolling. After reaching the yield point, a gradual increase in stresses to maximum values is observed, followed by a decrease due to strain localization. The character of the curve changes significantly after HPT. A decrease in the uniform strain, a significant increase in the strength parameters and a decrease in ductility are observed. High-temperature annealing of the deformed state leads to the development of recrystallization and complete leveling of the hardening effect from the formation of the UFG structure and distortions of the crystal lattice. Additional HPT leads to a rapid increase in the material strength but a significant loss of ductility. However, subsequent annealing at 350 °C to relieve the stresses provides an increase in ductility while maintaining high strength. A summary of the changes in mechanical properties is presented in Table 2.

As seen from Tables 1 and 2, the structural parameters of CP Ti Grade 4 differ significantly in various states and therefore may contribute differently to the strength properties of the material.

The contributions of various microstructural parameters to the overall strength of the material are important to be calculated for establishing the basic mechanisms of hardening after the combined deformation-heat treatment of CP Ti Grade 4, as well as for understanding the nature of its superstrength state. Following Refs.^[2,5,9,23], the calculation may be realized by considering the additive contribution of such strengthening mechanisms as grain boundary (σ_{gb}), dislocation (σ_{dis}), solid solution (σ_{ss}) and dispersion (σ_{Or}) strengthening to the flow stress:

$$\sigma_{total} = \sigma_0 + \sigma_{gb} + \sigma_{dis} + \sigma_{ss} + \sigma_{Or} \quad (2)$$

where $\sigma_0 \approx 80$ MPa and is the frictional stress of the crystal lattice in Ti^[15,24].

Following the known relations for these strengthening mechanisms [such as grain boundary hardening (Hall-Petch strengthening), dislocation hardening, solid solution and dispersion hardening (Orowan equation)] and considering the microstructural data in Table 2, the contributions of different strengthening mechanisms to UFG Ti strength were calculated. Their comparison with experimental data from mechanical tests is provided in Table 3.

Various strengthening mechanisms contribute to the strength of UFG Ti. However, their contributions in the state with the highest strength ($\sigma_T = 1340$ MPa) are noticeably less than this value, which means that the deformation of UFG Ti in such a state may also be affected by a different strengthening mechanism. Similar conclusions have been made for other UFG metallic materials, including Al alloys^[11,12] and a number of steels^[13,14]. Such a strengthening mechanism may be related to the state of grain boundaries in UFG materials, their non-equilibrium structure containing grain boundary dislocations and the grain boundary segregation of alloying elements^[10,25].

Recent model calculations in Ref.^[26] show [Figure 6] that the formation of segregations of impurities or alloying elements at grain boundaries may significantly inhibit the dislocation nucleation at grain boundaries, thereby contributing to the additional hardening of UFG materials. Simultaneously, computer simulations^[27,28] and experimental studies^[11,12,14,17-19] provide convincing evidence of the formation of grain

Table 1. Structural parameters of CP Ti Grade 4 after various processing regimes

State	Average grain size, d , μm	Total dislocation density, ρ , m^{-2}	Size of second-phase particles, r , nm	Volume fraction of second-phase particles, f , %
Hot rolled	10.00 ± 2.00	$\approx 2.4 \cdot 10^{14}$	10^3	2-3
HPT	0.12 ± 0.03	$\approx 2.1 \cdot 10^{15}$	-	<1
HPT + 700	5.00 ± 1.00	$\approx 2.2 \cdot 10^{14}$	35 ± 7	4-5
HPT + 700 + HPT	0.09 ± 0.03	$\approx 1.6 \cdot 10^{15}$	-	<1
HPT + 700 + HPT + 350	0.12 ± 0.04	$\approx 2.3 \cdot 10^{14}$	18 ± 10	7-8

Table 2. Mechanical properties of Ti Grade 4 in various structural states

State	Microhardness, HV	$\sigma_{0.2}$, MPa	σ_B , MPa	ϵ_f , %
Hot rolled	237 ± 2	500	680	23.9 ± 1.4
HPT	353 ± 7	1020	1170	8.9 ± 1.2
HPT + 700	266 ± 5	600	720	30.8 ± 2.0
HPT + 700 + HPT	423 ± 8	1200	1340	0.9 ± 0.4
HPT + 700 + HPT + 350	433 ± 3	1340	1510	9.5 ± 2.0

$\sigma_{0.2}$: Yield stress; σ_B : tensile strength; ϵ_f : elongation to failure.

Table 3. Calculated contributions of various strengthening mechanisms to the strength of UFG Ti Grade 4 and experimental data on yield strength values for all analyzed states

State	σ_{Tr} , MPa	$\sigma_{T\text{ calc}}$, MPa	σ_{Gr} , MPa	σ_{gb} , MPa	σ_{dis} , MPa	σ_{ss} , MPa	σ_{Or} , MPa	σ_{SL} , MPa
Hot rolled	500	480	80	140	150	110	0	0
HPT	1020	980		350	440		0	0
HPT+700	600	600		200	140		70	0
HPT + 700 + HPT	1200	1170		400	380		0	200
HPT + 700 + HPT + 350	1340	830		340	150		150	0

boundary segregations during the formation of UFG structures in metallic materials using SPD techniques. However, their nature and morphology are closely related to the processing regimes.

CONCLUSION

Recent studies show that the strength of UFG materials processed by SPD techniques is traditionally much higher than that predicted by the Hall-Petch relation. The physical nature of this phenomenon is related to the fact that the strength properties of UFG materials result not only from the presence of ultrafine grains but also from other nanostructural features, including the formation of subgrain dislocation structures, nanotwins, nanosized second-phase precipitations and the grain boundary structure, their non-equilibrium nature and the presence of grain boundary segregations of impurities or alloying elements. The latter factor is very important since it may contribute significantly to the strength of UFG materials. Moreover, the segregations at grain boundaries can also affect the ductility of such metals and alloys. In particular, as has recently been shown, the presence of grain boundary Zn in Al alloys with ultrafine grains leads to the phenomenon of superplasticity at lower temperatures^[27]. In this regard, the nature of grain boundary segregations and their behavior in deformation mechanisms is a relevant and exciting problem. The coming years may witness the study of strengthening mechanisms and their control using SPD techniques to become a relevant trend in the development of metallic materials with not only very high strength but also ductility and other enhanced mechanical properties.

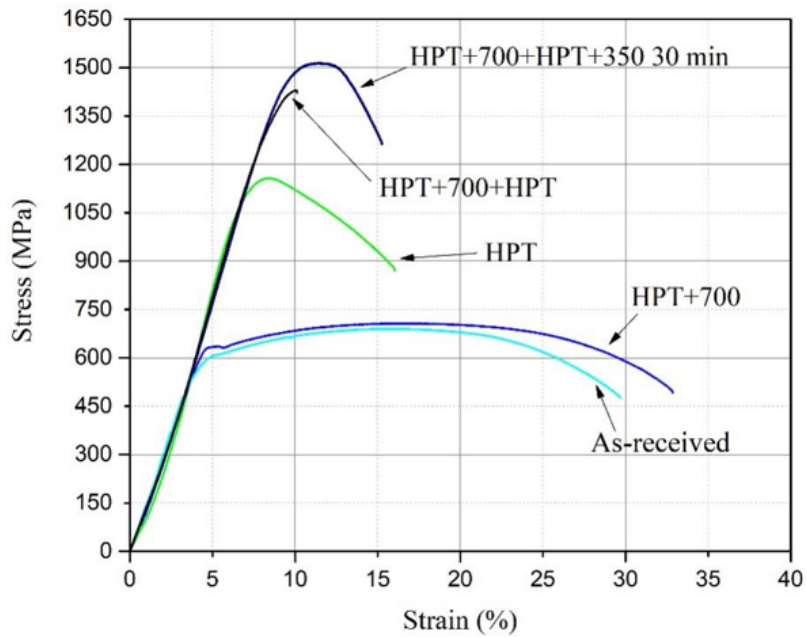


Figure 5. Engineering stress-strain curves of Ti Grade 4 after various treatments.

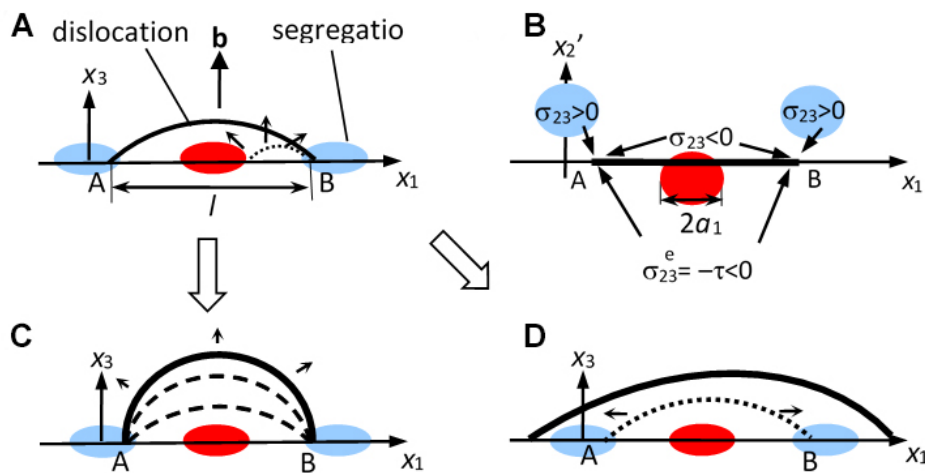


Figure 6. Expansion of a dislocation loop in the presence of segregations. The blue and red ovals denote the segregations that hinder and promote loop expansion, respectively. (A and B) Dislocation loop ends, A and B, which nucleate and expand under the action of the applied load, are pinned by segregations. (A) Projection on dislocation glide plane illustrating segregation-induced pinning. (B) Projection on grain boundary plane illustrating the fact that a segregation can either promote or hinder dislocation loop expansion, depending on the sign of the x_2 -coordinate of its center. (C) Dislocation loop expansion realized via its bow-out, thereby increasing the applied load if segregation-induced pinning is strong. (D) If pinning is weak, loop expansion is realized via the unpinning and lateral motion of points A and B. Reproduced with permission, Copyright 2019, Elsevier^[26].

DECLARATIONS

Acknowledgments

Author acknowledges the support in part from Russian Science Foundation (Grant No. 22-19-00445) and in part by the Ministry of Science and Higher Education of Russian Federation (Agreement No. 075-15-2022-1114 as of 06/30/2022). The Author also appreciates the Ministry of Science and Higher Education of the Russian Federation, the contract 075-15-2021-709, unique identifier of the project RF-2296.61321X0037, for

discussion of the results.

Authors' contribution

The author contributed solely to the article.

Availability of data and materials

The data and related materials of this study are available from the corresponding author on reasonable request.

Financial support and sponsorship

This work was supported by Russian Science Foundation (Grant No. 22-19-00445).

Conflicts of interest

The Author declare that there are no conflicts of interest.

Ethical approval and consent to participate

Not applicable.

Consent for publication

Not applicable.

Copyright

© The Author(s) 2023.

REFERENCES

1. Gleiter H. Nanostructured materials: basic concepts and microstructure. *Acta Mater* 2000;48:1-29. DOI
2. Meyers M, Mishra A, Benson D. Mechanical properties of nanocrystalline materials. *Prog Mater Sci* 2006;51:427-556. DOI
3. Valiev R, Islamgaliev R, Alexandrov I. Bulk nanostructured materials from severe plastic deformation. *Prog Mater Sci* 2000;45:103-89. DOI
4. Zehetbauer MJ, Zhu YT. (eds.). Bulk nanostructured materials. Weinheim, Germany: Wiley, 2009.
5. Valiev RZ, Zhilyaev AP, Langdon TG. Bulk nanostructured materials: fundamentals and applications. Hoboken: TMS-Wiley, 2014.
6. Firstov SA, Rogul TG, Shut OA. Transition from microstructures to nanostructures and ultimate hardening. *Funct Mater* 2009;16:364-373.
7. Horita Z, Edalati K. Severe plastic deformation for nanostructure controls. *Mater Trans* 2020;61:2241-7. DOI
8. Edalati K, Bachmaier A, Beloshenko VA, et al. Nanomaterials by severe plastic deformation: review of historical developments and recent advances. *Mater Res Lett* 2022;10:163-256. DOI
9. Ovid'ko I, Valiev R, Zhu Y. Review on superior strength and enhanced ductility of metallic nanomaterials. *Prog Mater Sci* 2018;94:462-540. DOI
10. Valiev RZ, Straumal B, Langdon TG. Using severe plastic deformation to produce nanostructured materials with superior properties. *Annu Rev Mater Res* 2022;52:357-82. DOI
11. Valiev R, Enikeev N, Murashkin M, Kazykhanov V, Sauvage X. On the origin of the extremely high strength of ultrafine-grained Al alloys produced by severe plastic deformation. *Scripta Mater* 2010;63:949-52. DOI
12. Liddicoat PV, Liao XZ, Zhao Y, et al. Nanostructural hierarchy increases the strength of aluminium alloys. *Nat Commun* 2010;1:63. DOI PubMed
13. Karavaeva MV, Kiseleva SK, Ganeev AV, et al. Superior strength of carbon steel with an ultrafine-grained microstructure and its enhanced thermal stability. *J Mater Sci* 2015;50:6730-8. DOI
14. Kim JG, Enikeev NA, Seol JB, et al. Superior strength and multiple strengthening mechanisms in nanocrystalline TWIP steel. *Sci Rep* 2018;8:11200. DOI PubMed PMC
15. Semenova I, Salimgareeva G, Da Costa G, Lefebvre W, Valiev R. Enhanced strength and ductility of ultrafine-grained Ti processed by severe plastic deformation. *Adv Eng Mater* 2010;12:803-7. DOI
16. Valiev R, Enikeev N, Langdon TG. Towards superstrength of nanostructured metals and alloys, produced by SPD. *Kovove Mater* 2021;49:1-9.
17. Abramova M, Enikeev N, Valiev R, et al. Grain boundary segregation induced strengthening of an ultrafine-grained austenitic stainless

- steel. *Mater Lett* 2014;136:349-52. [DOI](#)
18. Sauvage X, Wilde G, Divinski S, Horita Z, Valiev R. Grain boundaries in ultrafine grained materials processed by severe plastic deformation and related phenomena. *Mater Sci Eng A* 2012;540:1-12. [DOI](#)
 19. Sauvage X, Ganeev A, Ivanisenko Y, Enikeev N, Murashkin M, Valiev R. Grain boundary segregation in UFG alloys processed by severe plastic deformation: grain boundary segregation in UFG. *Adv Eng Mater* 2012;14:968-74. [DOI](#)
 20. Zhang Y, Jin S, Trimby PW, et al. Dynamic precipitation, segregation and strengthening of an Al-Zn-Mg-Cu alloy (AA7075) processed by high-pressure torsion. *Acta Mater* 2019;162:19-32. [DOI](#)
 21. Valiev RZ, Sabirov I, Zemtsova EG, Parfenov EV, Dluhoš L, Lowe TC. Nanostructured commercially pure titanium for development of miniaturized biomedical implants. In Froes F, Qian M, editors. *Titanium in medical and dental applications*. 1st ed. Sawston: Woodhead Publishing, 2018. p. 393-417.
 22. Rezyapova L, Valiev R, Sitdikov V, Valiev R. Study of second phase precipitates in nanostructured commercially pure titanium. *Lett Mater* 2021;11:345-50. [DOI](#)
 23. Balasubramanian N, Langdon TG. The Strength-grain size relationship in ultrafine-grained metals. *Metall Mater Trans A* 2016;47:5827-38. [DOI](#)
 24. Luo P, Hu Q, Wu X. Quantitatively analyzing strength contribution vs grain boundary scale relation in pure titanium subjected to severe plastic deformation. *Metall Mater Trans A* 2016;47:1922-8. [DOI](#)
 25. Valiev RZ. Superior strength in ultrafine-grained materials produced by SPD processing. *Mater Trans* 2014;55:13-8. [DOI](#)
 26. Bobylev S, Enikeev N, Sheinerman A, Valiev R. Strength enhancement induced by grain boundary solute segregations in ultrafine-grained alloys. *Int J Plast* 2019;123:133-44. [DOI](#)
 27. Chinh NQ, Murashkin MY, Bobruk EV, et al. Ultralow-temperature superplasticity and its novel mechanism in ultrafine-grained Al alloys. *Mater Res Lett* 2021;9:475-82. [DOI](#)
 28. Petrik MV, Kuznetsov AR, Enikeev NA, Gornostyrev YN, Valiev RZ. Peculiarities of interactions of alloying elements with grain boundaries and the formation of segregations in Al-Mg and Al-Zn Alloys. *Phys Met Metallogr* 2018;119:607-12. [DOI](#)